ARTICLE OPEN

Check for updates

The Exon Junction Complex component EIF4A3 plays a splicing-linked oncogenic role in pancreatic ductal adenocarcinoma

Ricardo Blázquez-Encinas[1,2,3], Emilia Alors-Pérez[1,2,3], María Trinidad Moreno-Montilla[1,2,3], Víctor García-Vioque[1,2,3], Marina Esther Sánchez-Frías[1,3,4], Andrea Mafficini[5,6], Juan L. López-Cánovas[1,2,3], Corinne Bousquet[7], Manuel D. Gahete[1,2,3,8], Rita T. Lawlor[5,6], Raúl M. Luque[1,2,3,8], Aldo Scarpa[6,9], Álvaro Arjona-Sánchez[1,3,10], Sergio Pedraza-Arevalo[1,2,3], Alejandro Ibáñez-Costa[1,2,3,11]✉ and Justo P. Castaño[1,2,3,8,11]✉

Pancreatic ductal adenocarcinoma (PDAC) is one of the most lethal cancers, underscoring the urgent need for in-depth biological research. The phenomenon of alternative RNA splicing dysregulation is a common hallmark in cancer, including PDAC, presenting new avenues for understanding and developing diagnostic and therapeutic tools. Our research focuses on EIF4A3, a core component of the Exon Junction Complex intimately linked to RNA splicing, and its role in PDAC. EIF4A3 is overexpressed in PDAC tissue and associated to clinical parameters of malignancy and poorer patient survival. Mechanistically, exploration of PDAC RNA-seq data unveiled the link of EIF4A3 to diverse malignancy processes, consistent with its association to key molecular pathways. EIF4A3 targeting in vitro decreased essential functional tumor features such as proliferation, migration, colony formation and sphere formation, while its in vivo targeting reduced tumor growth. *EIF4A3* silencing in PDAC cell lines severely altered its transcriptional and spliceosomic landscapes, as shown by RNA-seq analyses, suggesting a role for EIF4A3 in maintaining RNA homeostasis. Our results indicate that EIF4A3 dysregulation in PDAC has a pleiotropic regulatory role on RNA biology, influencing key cellular functions. This paves the way to explore its potential as novel biomarker and actionable target candidate for this lethal cancer.

Cancer Gene Therapy; https://doi.org/10.1038/s41417-024-00814-3

INTRODUCTION

Pancreatic ductal adenocarcinoma (PDAC) remains one of the most lethal cancers worldwide, mostly due to its late diagnosis—often with metastasis—and current lack of effective treatments, jointly leading to poor prognosis [1–3]. Research advances on PDAC molecular biology have established the primary pathologic relevance of the most frequently mutated genes: *KRAS*, *TP53*, *CDKN2A* and *SMAD4* [1, 2]. However, the knowledge gathered to date cannot fully explain the molecular underpinnings of the disease, and its present translation into clinical benefits for the patients is still lagging [2, 4–6]. Hence, novel research avenues are sorely required to find new molecular players that facilitate a better understanding of PDAC and provide new biomarkers and therapeutic targets to tackle this pathology. In this vein, studies from our group and others have shown that dysregulation of RNA splicing plays a key role in PDAC, which leverages this still limitedly known mechanism as a source of novel molecular tools [7–12].

Splicing is a process of RNA maturation that occurs co-transcriptionally, by which introns are removed from pre-RNA and exons are joined together [13]. This process is finely regulated to enable the generation of different mature RNA variants, or isoforms, from the same gene, which can then give rise to different proteins, or to mature non-translated RNAs [14], thereby increasing the diversity and versatility of the genome. Alternative splicing is therefore a capital step within the central dogma of Biology (DNA -> RNA -> protein) and its dysregulation is linked to the appearance of many diseases including cancer [15]. Altered splicing can lead to the generation of oncogenic splice variants and/or changes in signaling pathways, which contribute to cancer development, progression, aggressiveness, metastasis and drug resistance [16, 11].

RNA splicing is intimately intertwined with other processes involved in RNA biology, whose machineries often share molecular components and interact to ensure the correct maintenance of

[1]Maimonides Institute for Biomedical Research of Cordoba (IMIBIC), Córdoba, Spain. [2]Department of Cell Biology, Physiology, and Immunology, University of Córdoba, Córdoba, Spain. [3]Reina Sofia University Hospital, Córdoba, Spain. [4]Pathology Service, Reina Sofía University Hospital, Córdoba, Spain. [5]Department of Engineering for Innovation Medicine, Section of Innovation Biomedicine, University and Hospital Trust of Verona, Verona, Italy. [6]ARC-Net Research Centre, University and Hospital Trust of Verona, Verona, Italy. [7]INSERM UMR-1037, Cancer Research Center of Toulouse (CRCT), Team 'Labellisée Ligue Contre le Cancer', University of Toulouse, Toulouse, France. [8]CIBER Fisiopatología de la Obesidad y Nutrición (CIBERobn), Córdoba, Spain. [9]Department of Diagnostics and Public Health, Section of Pathology, University and Hospital Trust of Verona, Verona, Italy. [10]Surgery Service, Reina Sofia University Hospital, Córdoba, Spain. [11]These authors contributed equally: Alejandro Ibáñez-Costa, Justo P. Castaño. ✉email: b12ibcoa@uco.es; justo@uco.es

Received: 1 April 2024 Revised: 18 July 2024 Accepted: 22 July 2024
Published online: 04 September 2024

RNA processing and metabolism [17]. In this context, a paradigmatic mechanism is the Exon Junction Complex (EJC), a key interactive player that participates in, regulates, and interrelates several RNA-related processes such as splicing, RNA export from the nucleus, translation, m6A RNA methylation, and RNA degradation [18, 19]. A central protein of the EJC is EIF4A3, which together with MAGOH and RBM8A forms a trimeric core that interacts with many other proteins [18]. EIF4A3 is a DEAD box-family RNA helicase that shares high homology with other two genes from this family, *EIF4A1* and *EIF4A2*, which participate in translation initiation, and have been implicated in cancer [18, 20]. EIF4A3 does not participate in translation initiation, but its main function has long been related to the EJC [18], while an emerging number of additional functions, related to RNA biology, are being proposed for this molecule: from its early link to nonsense mediated decay (NMD) [21] to its recent bonds to ribosome biogenesis and m6A regulation [22], along with multiple associations with non-coding RNA regulation, including long non-coding RNA (lncRNA), circular RNA (circRNA), and micro RNAs (miRNA; [23], reviewed in [18]. Previous studies on the EIF4A family in PDAC mostly focused on EIF4A1/EIF4A2 and their role in translation initiation [24–26]. In contrast, few reports have examined the RNA metabolism-related functions of EIF4A3 in PDAC, where it was shown to mediate the actions of a lncRNA, LINC01232 [27] and a circRNA, circRNF13 [28]. Actually, the first identification of EIF4A3 in PDAC was unrelated to its currently known functions, but derived from a proteomic-based detection of Dead-box protein 48 (DDX48, an earlier name for EIF4A3) as an autoantigen in the sera of PDAC patients [29]. While it was proposed that the detection of autoantibodies to DDX48 could help improve PDAC diagnosis, no further reports confirmed or extended this idea. In other cancers, EIF4A3 has been found to be dysregulated and to play an oncogenic role and its underlying mechanisms have been examined [30–32]. Recently, we and others reported a profound alteration of key components of the splicing machinery in PDAC, with pathological implications [7–10, 12]. This prompted us to devise the present study, aimed at elucidating the role of *EIF4A3* in PDAC pathophysiology, with particular attention to its involvement as a regulator of alternative splicing.

MATERIAL AND METHODS

Patients and samples

Formalin-fixed paraffin embedded (FFPE) samples from 75 PDAC patients were used in this study (Discovery Cohort), obtaining tumor and non-tumor adjacent tissue from each of them. Clinical characterization of these patients has been recently reported in detail [12]. The use of human samples for this study was approved by the Ethics Committee of the Reina Sofia University Hospital of Córdoba (Spain) and the study has been conducted following Declaration of Helsinki principles.

Data from a separate cohort of 177 PDAC samples, obtained from the PanCancer study, were also used as Validation Cohort [33]. Clinical and gene expression data from these patients were downloaded from cBioportal [34, 35].

Cell culture

Two different model cell lines of PDAC were used in functional assays for this study: Capan-2 and MIAPaCa-2 (ATCC, Barcelona, Spain). Capan-2 cells were cultured in McCoy's 5A Medium (Gibco, Madrid, Spain) supplemented with 10% fetal bovine serum, 2 mM L-glutamine and 0.2% of antibiotic/antimycotic. MIAPaCa-2 cells were cultured in Dulbecco's Modified Eagle's Medium 4.5 g/L glucose supplemented with 10% fetal bovine serum, 2.5% horse serum, 2 mM L-glutamine and 0.2% of antibiotic/antimycotic. Both cell lines were cultured in a constant humidity 37 °C and 5% CO_2 atmosphere. Mycoplasma presence was checked weekly by PCR, as reported in [36].

RNA isolation, reverse transcription, quantitative PCR and qPCR microfluidic array

Total RNA was isolated from FFPE samples (Discovery Cohort) using Maxwell 16 LEV RNA FFPE Kit (Promega, Madrid, Spain), following manufacturer's instructions. In the samples of pancreatic human tumor tissues, expert pathologists delineated the regions that corresponded to tumor or adjacent non-tumor tissue, from which separate sections were subsequently obtained, as it has been described in detail in previous studies [12, 37–39]. RNA from cell lines was isolated using TRIzol reagent protocol. RNA was DNAse treated with RNAse-free DNAse kit (Qiagen, Milan, Italy) and it was further quantified using Nanodrop One spectrophotometer (Thermo Fisher Scientific, Madrid, Spain).

RNA was reverse transcribed using cDNA First Strand Synthesis kit (Thermo Fisher Scientific) with random hexamer primers. Gene expression was quantified using the previously published qPCR protocol [40] based on Brilliant III SYBR Green-qPCR MasterMix (Stratagene, La Jolla, CA, USA) in the Stratagene Mx3000p system.

To simultaneously measure the expression of *EIF4A3* in the Discovery Cohort samples, a dynamic microfluidic qPCR array was used, as previously published by our group [12, 41]. Biomark System and FluidigmVR Real-Time PCR Analysis Software v.3.0.2 and Data Collection Software v.3.1.2 (Fluidigm, South San Francisco, CA, USA) were used to extract and analyze the expression data, using *ACTB, GAPDH* and *HPRT* as housekeeping genes.

RNA-seq analysis from PDAC samples cohort

An additional Exploration Cohort of 94 samples of tumor tissue from patients with PDAC, comprising clinical and RNA-seq data (described in [12]), was used to explore the associations of *EIF4A3* expression with that of other genes and with the features and patterns of alternative splicing. To this aim, RNA-seq reads were pseudo-aligned and quantified using Salmon and GENCODE v34 version of the human transcriptome. Salmon quantification files were imported to R using Tximeta package. Gene expression was normalized using variance stabilizing transformation (VST) with DESeq2. Patient tumors were classified according to *EIF4A3* expression into three groups (high, intermediate and low *EIF4A3* expression samples) using mclust E model by mclust R package.

Alternative splicing events were quantified using SUPPA2 from Salmon quantification files. Briefly, Percent Spliced In (PSI) indexes were quantified for each of the events in the transcriptome detected in every sample (named "detected events"). Delta PSI (ΔPSI) was calculated for each event by comparing high and low *EIF4A3* expression groups, and p value was also calculated using Wilcoxon test, which compares the mean PSI of each event between the two groups. Events with p value < 0.05 were considered statistically significant and were named "*EIF4A3* associated events". Frequencies of each of the seven types of splice events detected by SUPPA2 (skipped exon, intron retention, mutually exclusive exons, alternative last exon, alternative first exon, alternative 5′ splice site and alternative 3′ splice site) were calculated for detected events and for EIF4A3 associated events, and then both distributions were compared by Fisher's exact test.

Gene silencing using specific siRNA

EIF4A3 expression was silenced in the cell lines using specific predesigned small interference RNAs (siRNA; #138378, Thermo Fisher Scientific). A Negative Control siRNA was also used (#4390843, Thermo Fisher Scientific). Specifically, cell lines were transfected using a mix of 30 nM concentration of siRNA and RNAiMax lipofectamine (Thermo Fisher Scientific), following manufacturer's instructions. Cells were detached after 48 h for further assays.

Proliferation assay

To study proliferation rate in response to *EIF4A3* silencing, resazurin assay was performed as previously reported [42]. Briefly, 3000 transfected cells/well were seeded in 96-well plates and serum starved for 24 h. After that, 10% resazurin medium was added and incubated for 3 h. Fluorescence (540 nm excitation/590 nm emission) was measured then, and the process was repeated after 24, 48 and 72 h at a FlexStation III system (Molecular Devices, Sunnyvale, CA, USA).

Migration assay

Migration capacity in response to *EIF4A3* silencing was tested using wound healing assay. Briefly, cells were seeded in 24-well plates and grown until total confluence and then a wound was made in the well with a pipette tip. Wells' medium was replaced by serum-free medium. Pictures were obtained at 0 and 24 h after wound was done to calculate the area recovered by the cells' migration. Pictures were analyzed with ImageJ software v.1.51 [43].

Colonies formation assay

Clonogenic assay was performed to evaluate the cells' ability to form colonies, as previously reported in detail [44]. Five thousand transfected cells per well were seeded in 6-well plates and were grown for 10 days. Cells were then fixed and stained with Crystal Violet (0.5%) and 6% formaldehyde solution. Pictures were obtained from the plates, and they were analyzed using ImageJ software v.1.51 [43].

Tumorspheres formation assay

Tumorspheres formation assay was performed as previously described [12], by seeding transfected cells in Corning Costar ultra-low attachment plates (#CLS3473, Merck, Madrid, Spain) in DMEM F-12 medium (#11320033, Gibco) supplemented with EGF (20 ng/ml) (#SRP3027, Sigma-Aldrich, Madrid, Spain) for 10 days. Pictures were obtained from the wells after 10 days of culture and analyzed using ImageJ software v.1.51 [43].

Xenografted mouse model

A basement membrane extract (#3432-010-01, Trevigen, Gaithersburg, MD, USA) suspension with 1 million MIAPaCa-2 cells was injected subcutaneously in each flank of a 7-weeks-old male athymic BALB/cAnNRj-Foxn1nu mouse (Janvier Labs, Le Genest-Saint-Isle, France). Tumor growth was measured with a digital caliper twice a week. After 15 days, *EIF4A3* and negative control siRNAs were injected in each of the flank tumors of the mice using AteloGene Reagent (#KKN1394, KOKEN Co, Tokyo, Japan). Tumor growth was measured twice a week for 2 weeks from the injection, when mice were sacrificed. These experiments were performed according to the European-Regulations for Animal-Care under the approval of the University of Cordoba research ethics committees.

RNA sequencing of silenced cell line

High quality RNA (RNA Integrity Number checked with Agilent BioAnalyzer) from MIAPaCa-2 cells was sequenced after transfecting with *EIF4A3* and negative control siRNAs ($n = 3$). RNA-seq was performed at the Centre for Genomic Regulation (CRG, Barcelona, Spain). Briefly, ribosomal RNA was depleted, the remaining RNA was fragmented, and library was prepared using Illumina kits. Paired-end sequencing was performed on a HiSeq2500 Illumina instrument to a yield of >50 million reads per sample. As previously described, FASTQ files were pseudoaligned and quantified using Salmon and gene expression analysis were performed using Tximeta and DESeq2.

For alternative splicing analysis, equivalent analysis was performed as described in the "RNA-seq analysis from PDAC samples cohort" section. Here, detected events were quantified from the MIAPaCa-2 cells, and EIF4A3 associated events were calculated by comparing *EIF4A3* silenced cells with the controls ($n = 3$).

Biocomputational and statistical analyses

All statistical analyses from cell lines experiments were performed using Prism 9 software (GraphPad Software, La Jolla, CA, USA). Normality distribution of continuous variables was checked using Shapiro–Wilk test. Mean values were compared using *t*-test, Mann–Whitney *U*-tests or one way ANOVA, depending on the result of data normality check and the number of groups to be compared. Correlation analyses were performed using Pearson tests. Protein interactome of EIF4A3 was established using STRING software, and Exon Junction Complex components were marked in the analysis according to Gene Ontology: Cellular Component term (GO:0035145). Gene expression analyses were performed with R version 4.1.0, using different packages for each analysis: survival_3.2-13 and survminer_0.4.9 for survival analysis, dnet_1.1.7 for gene enrichment analysis, pheatmap_1.0.12 for heatmap representation and ggplot_3.3.5 for graph visualization. Gene Set Enrichment Analyses (GSEA) were performed using GSEA_4.2.3 software. Significance was established at $p < 0.05$.

RESULTS

EIF4A3 is overexpressed in pancreatic ductal adenocarcinoma and associated with poor prognosis

EIF4A3 expression was measured by RT-qPCR microfluidic array in tumor and non-tumor adjacent tissues from 75 PDAC patients of the Discovery Cohort, showing an overexpression of this gene in tumor tissue at mRNA level (Fig. 1a). Receiver operating characteristic (ROC) curve analysis confirmed the capacity of *EIF4A3* expression levels to distinguish between tumor and non-tumor tissues, with an area under the curve (AUC) of 0.6129 (Supplementary Fig. 1a). Interestingly, comparing *EIF4A3* expression in tumor samples from the PanCancer study (TCGA) and healthy pancreas tissue from The Genotype-Tissue Expression (GTEx) confirmed a higher expression of *EIF4A3* in PDAC than in healthy pancreas tissue (Fig. 1b). Further, increased *EIF4A3* expression was associated to relevant clinical features, such as two types of tumor staging (higher in T4 and in stage III) and metastatic disease (Fig. 1c). Nevertheless, despite being statistically significant, we have to introduce the caveat that the differences found for grade T4 and stage III are more modest than robust, likely due to the comparatively lower number of advanced stage samples, as most of the patients in these advanced stages are less often candidate for surgery. TNM and stage are related, but not equivalent measures of tumor features that inform about distinct anatomopathological and clinical characteristics of the tumor. Most importantly, in the PanCancer dataset, *EIF4A3* expression was clearly associated to poorer Overall, Progression Free and Disease Specific survival of patients (Fig. 1d). Interestingly, however, *EIF4A3* expression was even associated to poorer Progression Free Survival when dividing the tumor samples in low stage (Stage I + Stage II) group and low TNM grading (T1 + T2) group separately, and also in high TNM grading (T3 + T4) group (Supplementary Fig. 1b). Unfortunately, high stage did not have enough samples to make the analysis.

EIF4A3 expression in PDAC is associated to distinct molecular pathways

To explore the molecular mechanisms associated to *EIF4A3* expression in PDAC, we explored RNA-seq data from another set of 94 tumor samples (Exploration Cohort). GSEA using Cancer Hallmarks Gene set (Fig. 2a) demonstrated that *EIF4A3* was associated to cell stress responses (UV response, Unfolded Protein response, Apoptosis), metabolic pathways (Glycolysis) and other signaling pathways that have been previously shown to be relevantly associated to PDAC pathophysiology (MTORC1, TNF-α or MYC). In line with this, enrichment analysis showed a direct correlation of *EIF4A3* mRNA levels in the tumors and the expression of many glycolysis-related genes (Fig. 2b). Furthermore, KEGG pathway analysis (Fig. 2c) exposed an association between *EIF4A3* expression and a number of metabolic pathways previously related to PDAC [45], from pyridine and purine metabolism to pentose phosphate pathway and to the metabolism of arginine, proline and other amino acids, as well as cell cycle. Interestingly, this analysis revealed an association of *EIF4A3* expression with the spliceosome pathway (Fig. 2c). Despite this pathway having the largest *p* value among the pathways shown, it was of particular interest due to its biological significance in the context of our study. We have previously described spliceosome dysregulation in PDAC, and EIF4A3 is part of the EJC, which is closely related to the splicing process [37, 46]. Additionally, we observed a particularly tight association with other core components of the EJC (as supported by protein interactome analysis in Supplementary Fig. 2), namely MAGOH, MAGOHB, and RBM8A (Fig. 2d).

Based on these correlations with the expression of multiple spliceosome components, we posited that the levels of *EIF4A3* expression could also be associated to distinctive patterns of alternative splicing. Interestingly, when comparing differential alternative splicing events between tumors expressing high and low *EIF4A3* levels, we found that skipping exons occur at a higher frequency in the EIF4A3 associated events than in the whole set of detected events (Fisher's exact test $p < 0.05$). Alternative 5′ and 3′ splicing sites events seem to be also more frequent, although their differences did not reach statistical significance (Fig. 2e). However,

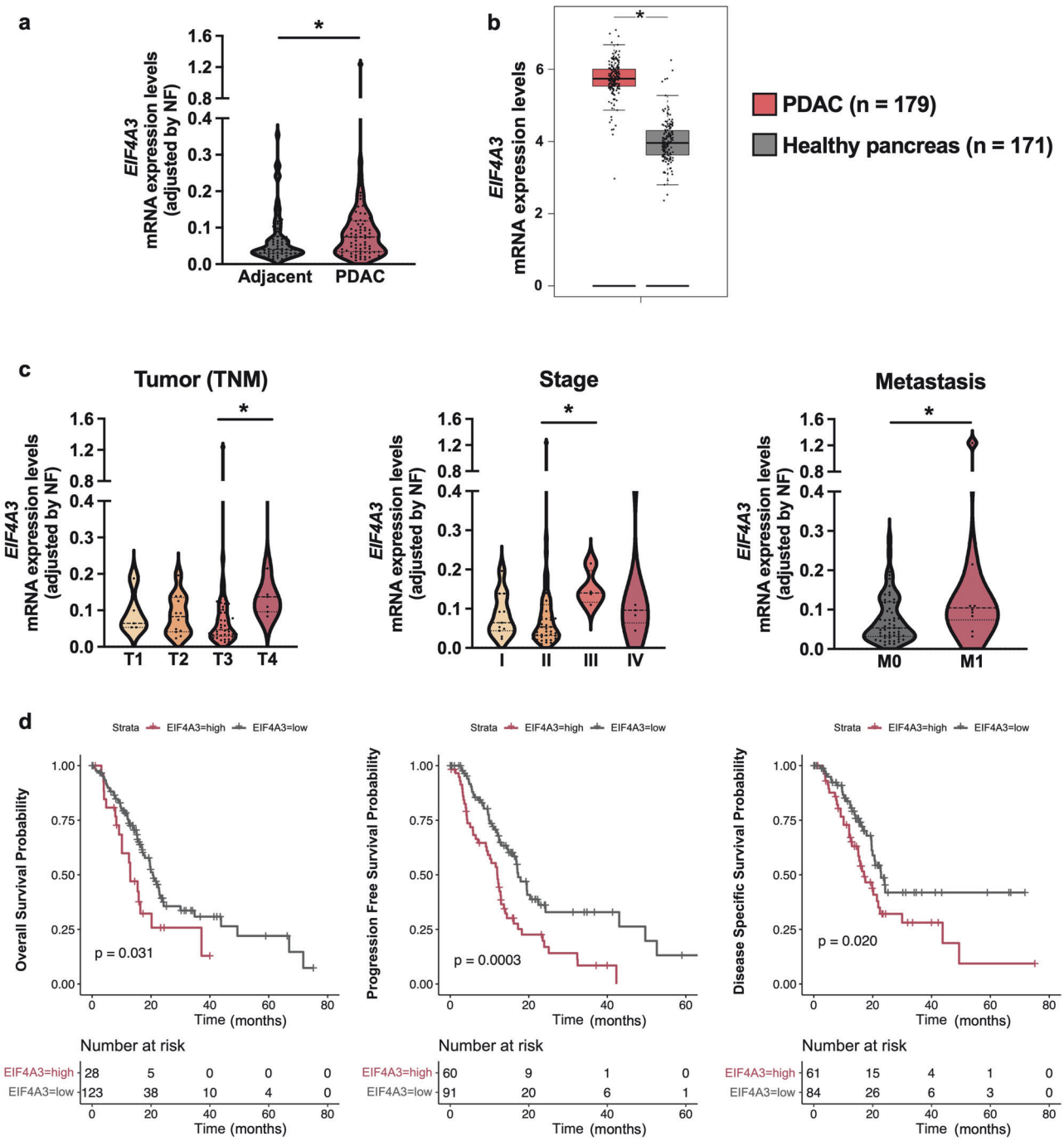

Fig. 1 Overexpression of *EIF4A3* in PDAC is associated with malignancy features. a *EIF4A3* expression in PDAC tumor tissue ($n = 73$) compared to non-tumor adjacent tissue ($n = 65$) as measured by qPCR microfluidic array in the Discovery Cohort. **b** *EIF4A3* expression in The Cancer Genome Atlas (TCGA) PDAC tumors ($n = 179$) compared to Normal Pancreas ($n = 171$) expression from The Genotype-Tissue Expression (GTEx). Graphic was obtained by GEPIA web server [62]. **c** Association of *EIF4A3* expression levels in tumor tissue to TNM stage (T1 $n = 5$, T2 $n = 12$, T3 $n = 44$, T4 $n = 7$), tumor stage (I $n = 11$, II $n = 49$, III $n = 4$, IV $n = 5$) and metastasis (M0 $n = 57$, M1 $n = 10$) in the Discovery Cohort. Data represent mean ± SEM. Mann–Whitney *U* test was used to compare means between two groups, and the Kruskal–Wallis test was used to compare means among more than two groups. When the Kruskal–Wallis test indicated significant differences, post hoc Dunn's test was employed to identify differences between groups pairs. Asterisks indicate significant differences (*$p < 0.05$). **d** Association of *EIF4A3* expression levels in tumor tissue to poorer overall, progression free and disease specific survival probability in PDAC patients from the PanCancer study. Logrank tests indicate statistical significance and *p* values are represented.

last exons events were less frequent among the EIF4A3 associated events (Fisher's exact test $p < 0.05$). First exons events also appeared to be less frequent (Fig. 2e). These results suggest a link between alteration of *EIF4A3* expression and alternative splicing dysregulation in PDAC.

EIF4A3 silencing decreases malignant functional features in vitro and in vivo

Based on the results described above, we hypothesized that decreasing *EIF4A3* expression could exert antitumor effects on PDAC. To test this notion, we used two model cell lines, Capan-2

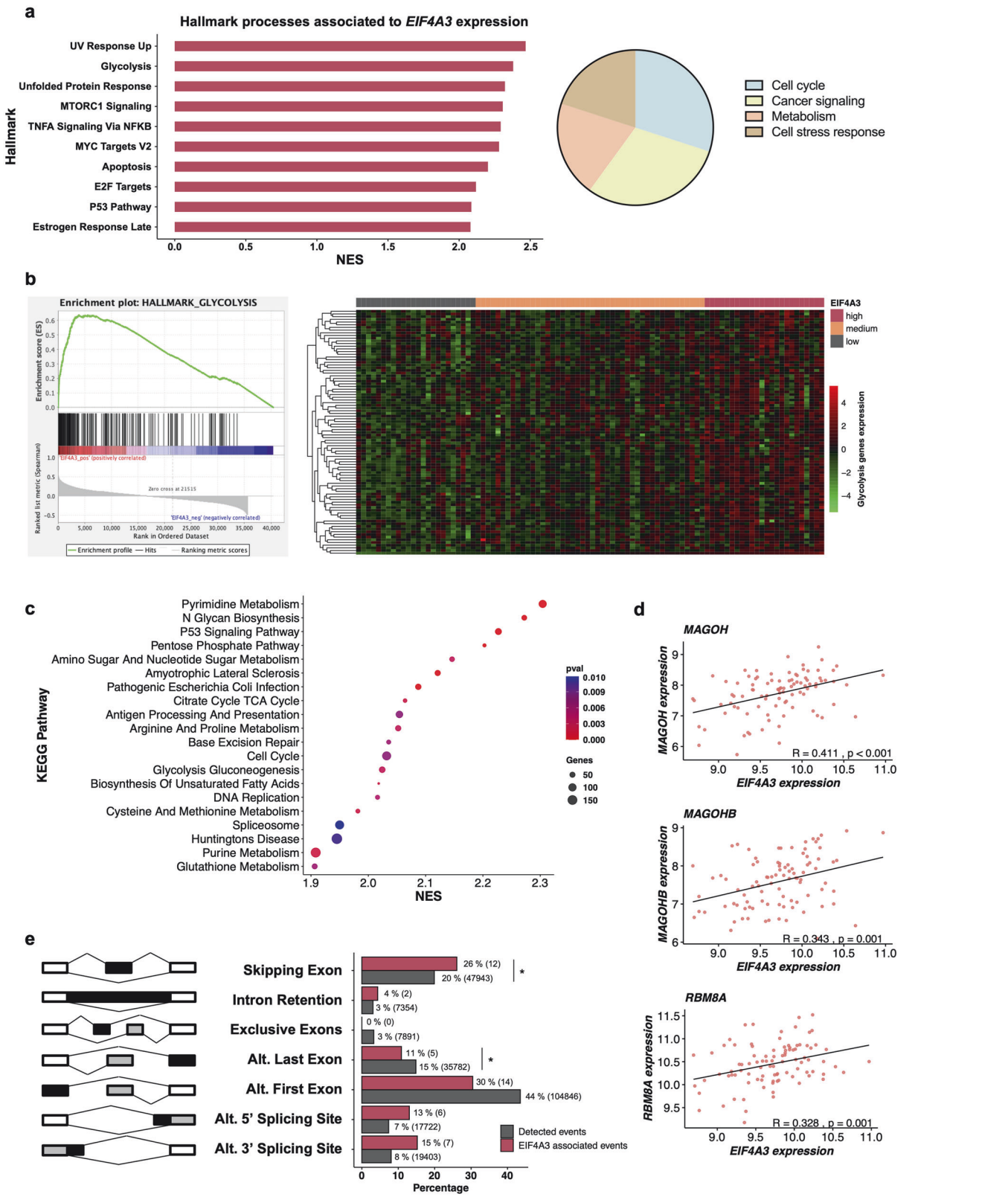

and MIAPaCa-2, where *EIF4A3* was silenced using either a specific siRNA (Supplementary Fig. 3) or a negative control siRNA (scramble). As illustrated in Fig. 3a, *EIF4A3* silencing decreased proliferation in both cell lines, although it was noteworthy that the effect was more apparent and time-dependent in the more aggressive and poorly differentiated MIAPaCa-2 cells, than in the well differentiated Capan-2 cells, which only reduced their proliferation at 72 h. Migration capacity of MIAPaCa-2 cells was also assessed in response to *EIF4A3* silencing by wound healing assay, where a clear decrease in the recovery of the wound at 24 h

Fig. 2 Analysis of *EIF4A3* expression in relation to PDAC molecular landscape in the Exploration Cohort. a Analysis of cancer hallmarks significantly associated to *EIF4A3* expression. Normalized enrichment score (NES) is plotted against hallmarks terms. Hallmarks terms were grouped in the pie chart according to their belonging to cell cycle, cancer signaling, metabolism or cell stress response (right). **b** Enrichment plot showing glycolysis hallmark associated to *EIF4A3* expression (left) and non-hierarchical heatmap showing the expression of glycolysis genes in low, intermediate, and high *EIF4A3* expression PDAC samples (right). **c** Analysis of KEGG pathways significantly associated to *EIF4A3* expression. NES is plotted against KEGG pathways, dot size represents the genes hits and dot colors represents *p* value of that pathway. **d** *EIF4A3* expression Pearson correlation to the other components of the Exon Junction Complex. **e** Bar plot showing the frequency from each alternative splicing event type detected in PDAC tumors (gray) and from those statistically associated to *EIF4A3* expression (red). Differences in the proportion of each splicing event were calculated using Fisher's exact test. Asterisks indicate significant differences (*$p < 0.05$).

was observed (Fig. 3b). Capan-2 cells could not be tested by this method because of their growing pattern at full confluence, which does not allow to use this assay.

Colony formation was also assessed after *EIF4A3* silencing (Fig. 3c), and a profound decrease was observed in both cell lines compared to scramble controls. Once again, the effect was stronger in MIAPaCa-2 cells, suggesting a particular link between this gene and stem cell properties in highly aggressive cells. Similar to colony formation, when tumorspheres formation capacity was tested in both cell lines, a decrease in the density of spheres formation was observed in response to *EIF4A3* silencing, when compared to scramble controls (Fig. 3d).

To further evaluate if the effects of *EIF4A3* silencing were also recapitulated in vivo, a xenograft model was generated by subcutaneous injection of MIAPaCa-2 cells in both flanks of athymic mice ($n = 6$). In each of the two tumors formed, we injected *EIF4A3* or scramble siRNAs as a negative control. After siRNAs injection, a decrease in tumor volume was observed only in tumors that received the *EIF4A3* silencing treatment (Fig. 3e). The difference in tumor volume increased over time and became statistically significant at 14 days. These results indicate that *EIF4A3* silencing has antitumor capacity not only in vitro but also in vivo.

EIF4A3 silencing alters gene expression of key molecular pathways

To explore the mechanistic underpinnings of *EIF4A3* silencing, we carried out an RNA-seq experiment with MIAPaCa-2 cells transfected with either *EIF4A3* or scramble siRNAs ($n = 3$). A robust (>50%) *EIF4A3* silencing was confirmed after the sequencing (Fig. 4a). Overall, 191 genes were upregulated (14 with fold-change >1.5), and 138 genes were downregulated (16 with fold-change <1.5) in *EIF4A3* silenced cells (Fig. 4b). To identify the molecular pathways these genes belong to, we performed two analyses. First, Hallmarks Gene Set Analysis (Fig. 4c) showed that there was an upregulation of MYC targets and oxidative phosphorylation genes, whereas other pathways like pancreas beta cells genes, the relevant KRAS signaling and TNF-α signaling sets, or immunity related gene sets like allograft rejection and complement, were downregulated. Further, KEGG pathways analysis revealed that after *EIF4A3* silencing, the main altered pathways were related to RNA processing and metabolic pathways (Fig. 4d). Overall, the main pathways associated to *EIF4A3* expression observed previously in the analysis of human samples (Fig. 2) and those altered after its silencing in MIAPaCa-2 cells substantially overlapped, as the latter related to carbon metabolism (oxidative phosphorylation) (Fig. 4e) and spliceosome (including EJC components *MAGOH* and *MAGOHB*) (Fig. 4f), which were both upregulated after *EIF4A3* silencing; and TNF-alpha signaling (Fig. 4g), which was repressed after *EIF4A3* silencing. Additionally, evaluation of a set of genes selected from the functional pathways found to be altered in Fig. 4e–g were further tested by qPCR. Notably, results from this assay confirming the predicted alteration in six out of the eight genes evaluated (Supplementary Fig. 4), thus lending additional support to the notion that altered *EIF4A3* expression is linked to changes in the expression of functionally relevant genes in pancreatic cancer.

EIF4A3 silencing modifies alternative splicing pattern in PDAC cells

Analysis of alternative splicing in RNA-seq data from MIAPaCa-2 transfected cells revealed that 280 genes were differentially spliced when *EIF4A3* was silenced, while, in contrast, most of them did not change in their expression levels (Fig. 5a). Remarkably, there were 535 alternative splicing events that changed their PSI (Wilcoxon test $p < 0.05$) when *EIF4A3* was silenced (Fig. 5b). Those events mainly belong to skipping exon and alternative first exon types, according to SUPPA2 analysis. Also, the pattern of EIF4A3 associated events (Fig. 5c) was different from that of the whole set of alternative splicing events detected, being skipping exon or alternative 3′ splice site overrepresented among the EIF4A3 associated events (Fisher's exact test $p < 0.05$), whereas alternative first and last exons and mutually exclusive exons were less frequently altered (Fisher's exact test $p < 0.05$). Additional enrichment analyses were performed to identify which genes were affected by the changes in alternative splicing pattern. Biological process Gene Ontology (GO) analysis showed that silencing *EIF4A3* mainly affected RNA translation and apoptosis related genes (Fig. 5d). Collectively, these results strongly suggest a relevant role for EIF4A3 in the selective regulation of alternative splicing events influencing capital biological functions in PDAC.

DISCUSSION

Pioneer reports showing two decades ago an altered expression of abnormal CD44 variants and other "spliceoforms" in PDAC [47] heralded the current bloom of experimental evidence supporting a major role of splicing dysregulation in this deadly cancer [11]. Subsequent work reinforced this notion by showing that the splicing machinery itself is dysregulated in PDAC, and can thereby contribute to trigger some of its typical pathological features, from its precursor pancreatitis [10], to increased cell proliferation and metastasis [9, 12], reviewed in [11]. Further, recent evidence is helping to dissect key molecular players that interact with and mediate the pathological impact of dysregulated splicing components, such as hnRNPK [8], SF3B1 [12], RBFOX2 [9], SRSF1 [10], and others, including core oncogenic hallmarks of PDAC like KRAS and TP53 [2]. In this context, there is still a notable dearth of knowledge on the potential role in PDAC of molecular players and mechanisms that, like the EJC component EIF4A3, are essential to maintain RNA homeostasis and splicing itself, and are involved in cancer [17–19]. In this scenario, our present study provides original evidence that EIF4A3 is altered in PDAC, where it associates to clinical and molecular features, and may serve a pathological role, mechanistically linked to the alteration of multiple pathways related to both metabolic routes and splicing and RNA biology.

Our initial interest on EIF4A3 was sparked by its involvement in splicing and by the growing evidence of its role in several cancers, which contrasted with the limited information available in PDAC. In fact, detailed studies have shown a relevant role of two

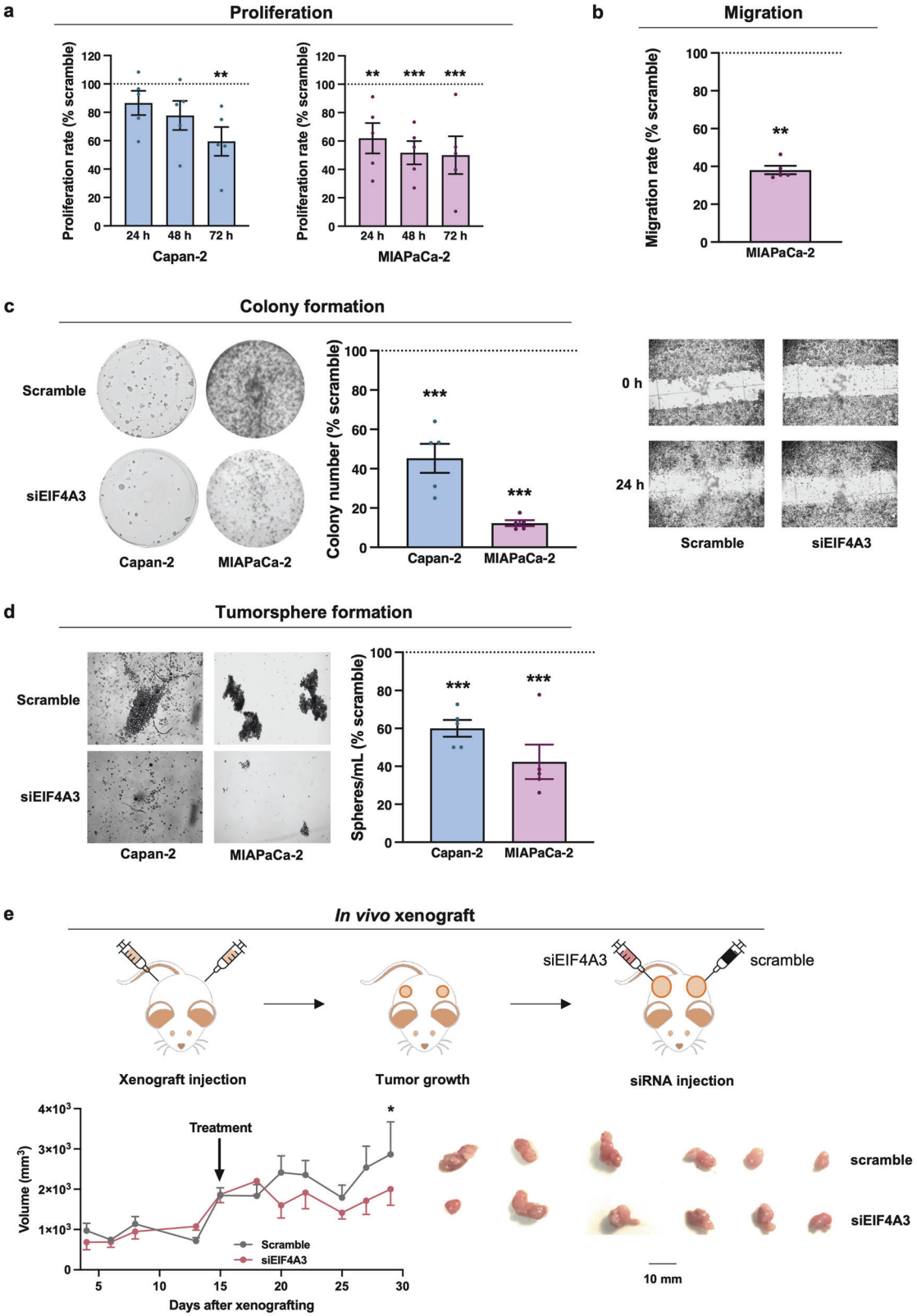

members of the EIF4A family, EIF4A1 and EIF4A2, in PDAC, where they seem to participate in the translational control of pancreatic tumor metabolism, a dependency potentially exploitable therapeutically [24, 25]. A similar metabolic link was reported for EIF4A1 and a related family member, EIF4E, in relation to phosphoglycerate dehydrogenase and translation initiation in PDAC [48]. However, few studies have explored EIF4A3 in PDAC and were focused on its interaction with other molecular players [27, 28]. In contrast, a growing number of studies are providing detailed experimental support for a relevant role of EIF4A3 in

Fig. 3 Functional effects of EIF4A3 targeting in PDAC models. a Proliferation rates of Capan-2 and MIAPaCa-2 cell lines in response to *EIF4A3* silencing at 24, 48 and 72 h compared to scramble silenced cells ($n = 5$). Mean differences were assessed using ANOVA, with post hoc Tukey's test to compare between group pairs. **b** Migration rate of MIAPaCa-2 cells in response to *EIF4A3* silencing compared to scramble silenced cells set at 100% ($n = 5$). Representative images are shown below. **c** Colony formation capacity of Capan-2 and MIAPaCa-2 cells in response to *EIF4A3* silencing compared to scramble silenced cells set at 100% ($n = 5$). Representative images are shown at the left. **d** Tumorsphere formation capacity of Capan-2 and MIAPaCa-2 cells in response to *EIF4A3* silencing compared to scramble silenced cells set at 100% ($n = 5$). Representative images are shown at the left. **e** EIF4A3 targeting reduces tumor volume in vivo ($n = 6$). At top panel, scheme of the xenograft experiment carried out; at bottom-left panel, volume of the tumors (*EIF4A3* and scramble silenced groups) during the full experiment; at bottom-right panel, a picture of the tumors after the mice sacrifice. Data represent mean ± SEM. Mean differences were assessed using *t*-test for (**b**–**e**). Asterisks indicate significant differences (*$p < 0.05$; **$p < 0.01$; ***$p < 0.001$).

various cancers, including hepatocellular carcinoma [30], breast cancer [31] cervical cancer [32] or glioblastoma [49, 50] (reviewed in [18]). Although the underlying mechanisms proposed to mediate EIF4A3 differ for each tumor type investigated, there is a common trend involving RNA-related molecules and processes [18]. In PDAC, EIF4A3 has been proposed to participate in the biogenesis of an oncogenic circRNA (circRNF13) in relation to the hypoxia-inducible factor-1 (HIF-1), a key player in aerobic glycolysis [28]. In turn, circRNF13 would promote cell proliferation, angiogenesis, invasion and glycolysis in PDAC cells and mice models by acting as a sponge for miR-654-3p and thereby augmenting the levels of pyruvate dehydrogenase kinase 3 (PDK3) [28]. On a distinct but related setting, EIF4A3 was recently proposed to mediate the oncogenic effect on PDAC of the long non-coding RNA LINC01232, which, after being induced by the ubiquitous transcription factor SP1, would recruit EIF4A3 to upregulate expression of the transmembrane 9 superfamily member 2 (TM9SF2) by enhancing its mRNA stability [27]. These studies document EIF4A3 as a relevant conduit mediating the actions of RNA-related actors in PDAC. However, they could not provide a more general vision of its role in this cancer.

By specifically focusing on the role and implications of EIF4A3 itself, our present work uncovered original evidence suggestive of an overarching regulatory role of this factor in PDAC, providing novel insights on its plausible influence at crossroads of metabolic routes, splicing and RNA biology. Indeed, *EIF4A3* expression levels showed tight links to glycolysis and several of its associated metabolic pathways, which are well known pivotal actors for PDAC oncogenesis and progression [2], not only in association studies in human PDAC samples but also after experimentally-driven causative modifications in cell lines. These findings are in line with reports on the ability of EIF4A3 to enhance biogenesis of glycolysis-inducing circRNAs in PDAC [28] and prostate cancer [51]. Interestingly, glycolysis activation in PDAC is known to be related to c-MYC [52], which has been proven to be persistently and aberrantly activated in this cancer [53, 54]. In turn, MYC hyperactivation is associated to dysregulation of key components of the splicing machinery in PDAC like SRSF1 [10]. In this scenario, our data showing a close correlation of *EIF4A3* expression with that of MYC- and glycolysis-related pathways in PDAC reinforce the emerging connection of MYC hyperactivation with splicing and metabolic dysregulation in cancer [10, 51, 55]. In a related metabolic context, we found that *EIF4A3* silencing enhanced expression of oxidative phosphorylation genes, suggesting a change in central carbon metabolism, which is known to be altered in PDAC, where it has been recently proposed as an anti-mitochondrial respiration therapy in specific patients [56]. Of note, our data also unveils that *EIF4A3* expression in PDAC is closely associated to several pathways classically linked to stress response, from apoptosis to UV response or Unfolded Protein response, which nicely fits a general (not just cancer-related) stress-linked function recently proposed for this molecule [57]. Nonetheless, the associations of EIF4A3 expression levels were not circumscribed to metabolic or splicing pathways, but also involved other pivotal factors in PDAC, such as TNF-α, which has been proposed as a potential therapy in this pathology [58, 59]. Specifically, *EIF4A3* silencing decreased the expression of TNF-α signaling pathway genes, including TNF-α itself, thereby implying putative interactions with PDAC microenvironment and metastasis [58, 60].

A particular novelty of our study is the discovery of the clear influence of *EIF4A3* expression on the global patterns of splicing in PDAC and how this translates to selective changes in specific gene families. Actually, the lack of information in this regard in PDAC was somewhat surprising, given the known roles of EIF4A3, as EJC component, in linking splicing with other processes like RNA export, NMD, and global RNA homeostasis [18, 46]. Interestingly, our data revealed that the increased expression levels of *EIF4A3* in human PDAC samples is associated to markedly altered patterns of alternative splicing. Moreover, experimental *EIF4A3* silencing in PDAC cells, rather than simply altering gene expression patterns, caused profound changes in alternative splicing profiles, which, in keeping with previous reports on EIF4A3 and the EJC, particularly involved skipping exons events [61]. Indeed, we observed that exon skipping and alternative 3′ splice site usage are the type of splicing events most commonly associated with alteration of *EIF4A3* expression in human samples. Additionally, these types of events are more affected when *EIF4A3* is silenced. In contrast, alternative first and last exons seem to be less dependent on *EIF4A3* expression. Detailed analysis of the molecular pathways affected by alternative splicing changes mediated by *EIF4A3* downregulation suggested a putative involvement of this factor in the regulation of cellular processes essential in cancer progression, such as those affecting apoptosis, NMD and RNA translation [17, 22]. These observations suggest that EIF4A3 would not only participate in the regulation of correct RNA metabolism but may also influence PDAC cell survival, disclosing its potential as an actionable target. In line with this notion, our in vitro and in vivo results demonstrated the functional therapeutic benefits of targeting *EIF4A3*. Specifically, its silencing in vitro reduced aggressiveness parameters (proliferation and migration rates) of PDAC cell lines, and reduced stemness functional parameters (colony and tumorspheres formation). Likewise, *EIF4A3* silencing blunted tumor growth in a preclinical model (MIAPaCa-2 derived xenografted mouse). Our results are in close agreement with recent reports showing that targeting EIF4A3 can reduce tumor growth or aggressiveness features in other cancer types [30–32, 49–51], reviewed in [18], thereby leveraging its potential as an actionable target in cancer.

In conclusion, our results indicate that the EJC component *EIF4A3* is abnormally overexpressed in PDAC, where it associates to malignant clinical features and poor patient survival. In line with the increasingly ample and relevant functions reported for EIF4A3, we found that this factor may play multiple roles in PDAC, involving from key metabolic pathways (glycolysis, oxidative phosphorylation) to RNA translation, NMD and, particularly splicing, thereby suggesting its potential as an overarching hub for the homeostasis of RNA biology. Finally, experimental in vitro and in vivo targeting of EIF4A3 decreased aggressiveness features and tumor growth of PDAC cells, providing primary evidence of its potential as a candidate therapeutic target in this dismal cancer.

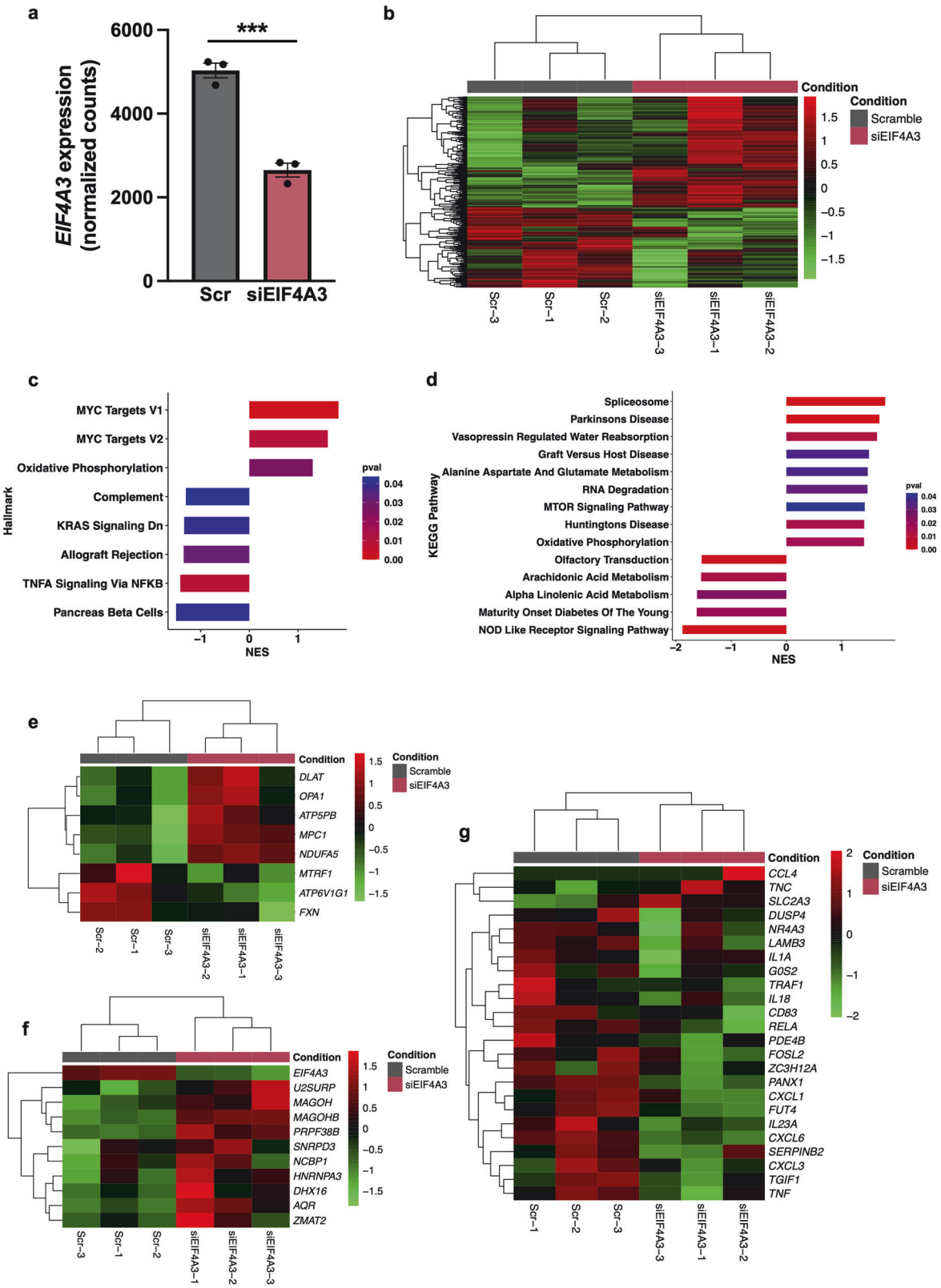

Fig. 4 Changes in the transcriptional profile of MIAPaCa-2 cells in response to *EIF4A3* silencing. a Normalized *EIF4A3* expression—as VST counts from DESeq2—in scramble vs. *EIF4A3* silenced MIAPaCa-2 cells ($n = 3$). Data represent mean ± SEM. Mean differences were assessed using *t*-test. Asterisks indicate significant differences (***$p < 0.001$). **b** Heatmap showing the differentially expressed genes (DEG) by DESeq2 in scramble vs. *EIF4A3* silenced MIAPaCa-2 cells. **c** Analysis of Hallmarks altered due to *EIF4A3* silencing in MIAPaCa-2 cells. Normalized enrichment score (NES) is positive for hallmarks enriched in *EIF4A3* silenced cells and NES is negative for those enriched in scramble silenced cells. Bars color represents *p* value for each pathway. **d** Analysis of KEGG pathways altered due to *EIF4A3* silencing in MIAPaCa-2 cells. NES is positive for hallmarks enriched in *EIF4A3* silenced cells and NES is negative for those enriched in scramble silenced cells. Bars color represents *p* value for each pathway. Heatmap showing the DEG expression from the oxidative phosphorylation (**e**), the spliceosome (**f**) and the TNF-α (**g**) pathways.

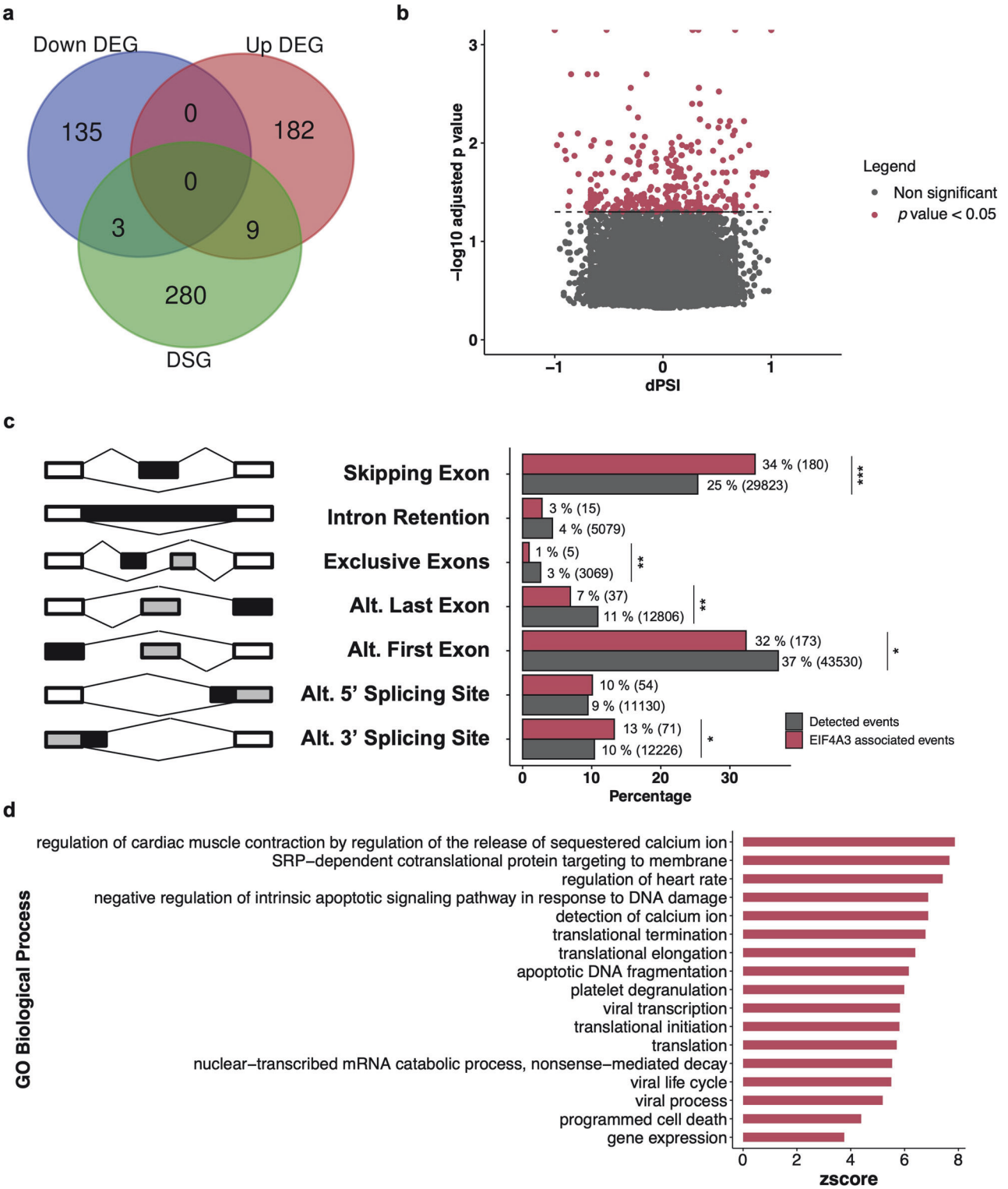

Fig. 5 Changes in alternative splicing in MIAPaCa-2 cells associated to *EIF4A3* silencing. a Venn diagram showing the intersection among the downregulated DEG, upregulated DEG and the differentially spliced genes (DSG) after *EIF4A3* silencing. **b** Volcano plot showing the differentially alternative splice events after *EIF4A3* silencing in MIAPaCa-2 cells. Differential Percent Splice In (dPSI) from each event is plotted against the logarithm of its *p* value. Those events with $p < 0.05$ are colored. **c** Bar plot showing the frequency from each alternative splicing event type detected in MIAPaCa-2 cells (gray) and from those statistically differential after *EIF4A3* silencing (red). Differences in the proportion of each splicing event were calculated using Fisher's exact test. Asterisks indicate significant differences (*$p < 0.05$; **$p < 0.01$; ***$p < 0.001$). **d** Analysis of Biological Process Gene Ontology (GO-BP) pathways enriched for the genes that were alternatively spliced after *EIF4A3* silencing ($p < 0.05$). *Z*-score is plotted for each of the GO-BP pathways. Only those pathways with adjusted *p* value < 0.01 are represented.

DATA AVAILABILITY

The datasets used and/or analyzed during the current study are available from the corresponding author upon reasonable request.

REFERENCES

1. Grossberg AJ, Chu LC, Deig CR, Fishman EK, Hwang WL, Maitra A, et al. Multidisciplinary standards of care and recent progress in pancreatic ductal adenocarcinoma. CA Cancer J Clin. 2020;70:375–403.
2. Halbrook CJ, Lyssiotis CA, Pasca di Magliano M, Maitra A. Pancreatic cancer: advances and challenges. Cell. 2023;186:1729–54.
3. Sung H, Ferlay J, Siegel RL, Laversanne M, Soerjomataram I, Jemal A, et al. Global Cancer Statistics 2020: GLOBOCAN estimates of incidence and mortality worldwide for 36 cancers in 185 countries. CA Cancer J Clin. 2021;71:209–49.
4. Bailey P, Chang DK, Nones K, Johns AL, Patch AM, Gingras MC, et al. Genomic analyses identify molecular subtypes of pancreatic cancer. Nature. 2016;531:47–52.
5. Waddell N, Pajic M, Patch AM, Chang DK, Kassahn KS, Bailey P, et al. Whole genomes redefine the mutational landscape of pancreatic cancer. Nature. 2015;518:495–501.
6. Connor AA, Gallinger S. Pancreatic cancer evolution and heterogeneity: integrating omics and clinical data. Nat Rev Cancer. 2022;22:131–42.
7. Wang J, Dumartin L, Mafficini A, Ulug P, Sangaralingam A, Alamiry NA, et al. Splice variants as novel targets in pancreatic ductal adenocarcinoma. Sci Rep. 2017;7:2980.
8. Escobar-Hoyos LF, Penson A, Kannan R, Cho H, Pan CH, Singh RK, et al. Altered RNA splicing by mutant p53 activates oncogenic RAS signaling in pancreatic cancer. Cancer Cell. 2020;38:198–211.e8.
9. Jbara A, Lin KT, Stossel C, Siegfried Z, Shqerat H, Amar-Schwartz A, et al. RBFOX2 modulates a metastatic signature of alternative splicing in pancreatic cancer. Nature. 2023;617:147–53.
10. Wan L, Lin KT, Rahman MA, Ishigami Y, Wang Z, Jensen MA, et al. Splicing factor SRSF1 promotes pancreatitis and KRASG12D-mediated pancreatic cancer. Cancer Discov. 2023;13:1678–95.
11. Alors-Pérez E, Pedraza-Arevalo S, Blázquez-Encinas R, Moreno-Montilla MT, García-Vioque V, Berbel I, et al. Splicing alterations in pancreatic ductal adenocarcinoma: a new molecular landscape with translational potential. J Exp Clin Cancer Res. 2023;42:282.
12. Alors-Perez E, Blázquez-Encinas R, Alcalá S, Viyuela-García C, Pedraza-Arevalo S, Herrero-Aguayo V, et al. Dysregulated splicing factor SF3B1 unveils a dual therapeutic vulnerability to target pancreatic cancer cells and cancer stem cells with an anti-splicing drug. J Exp Clin Cancer Res. 2021;40:382.
13. Marasco LE, Kornblihtt AR. The physiology of alternative splicing. Nat Rev Mol Cell Biol. 2023;24:242–54.
14. Wright CJ, Smith CWJ, Jiggins CD. Alternative splicing as a source of phenotypic diversity. Nat Rev Genet. 2022;23:697–710.
15. Bradley RK, Anczuków O. RNA splicing dysregulation and the hallmarks of cancer. Nat Rev Cancer. 2023;23:135–55.
16. Wang E, Aifantis I. RNA splicing and cancer. Trends Cancer. 2020;6:631–44.
17. Wolin SL, Maquat LE. Cellular RNA surveillance in health and disease. Science. 2019;366:822–7.
18. Ye J, She X, Liu Z, He Z, Gao X, Lu L, et al. Eukaryotic initiation factor 4A-3: a review of its physiological role and involvement in oncogenesis. Front Oncol. 2021;11:712045.
19. Woodward LA, Mabin JW, Gangras P, Singh G. The exon junction complex: a lifelong guardian of mRNA fate. Wiley Interdiscip Rev RNA. 2017;8:e1411.
20. Xue C, Gu X, Li G, Bao Z, Li L. Expression and functional roles of eukaryotic initiation factor 4A family proteins in human cancers. Front Cell Dev Biol. 2021;9:711965.
21. Gehring NH, Kunz JB, Neu-Yilik G, Breit S, Viegas MH, Hentze MW, et al. Exon-junction complex components specify distinct routes of nonsense-mediated mRNA decay with differential cofactor requirements. Mol Cell. 2005;20:65–75.
22. Kanellis DC, Espinoza JA, Zisi A, Sakkas E, Bartkova J, Katsori AM, et al. The exon-junction complex helicase eIF4A3 controls cell fate via coordinated regulation of ribosome biogenesis and translational output. Sci Adv. 2021;7:eabf7561.
23. Li Y, Ren S, Xia J, Wei Y, Xi Y. EIF4A3-induced circ-BNIP3 aggravated hypoxia-induced injury of H9c2 cells by targeting miR-27a-3p/BNIP3. Mol Ther Nucleic Acids. 2020;19:533–45.
24. Müller D, Shin S, Goullet de Rugy T, Samain R, Baer R, Strehaiano M, et al. eIF4A inhibition circumvents uncontrolled DNA replication mediated by 4E-BP1 loss in pancreatic cancer. JCI Insight. 2019;4:e121951.
25. Chan K, Robert F, Oertlin C, Kapeller-Libermann D, Avizonis D, Gutierrez J, et al. eIF4A supports an oncogenic translation program in pancreatic ductal adenocarcinoma. Nat Commun. 2019;10:5151.
26. Singh K, Lin J, Lecomte N, Mohan P, Gokce A, Sanghvi VR, et al. Targeting eIF4A dependent translation of KRAS signaling molecules. Cancer Res. 2021;81:2002–14.
27. Li Q, Lei C, Lu C, Wang J, Gao M, Gao W. LINC01232 exerts oncogenic activities in pancreatic adenocarcinoma via regulation of TM9SF2. Cell Death Dis. 2019;10:698.
28. Zhao Q, Zhu Z, Xiao W, Zong G, Wang C, Jiang W, et al. Hypoxia-induced circRNF13 promotes the progression and glycolysis of pancreatic cancer. Exp Mol Med. 2022;54:1940–54.
29. Xia Q, Kong XT, Zhang GA, Hou XJ, Qiang H, Zhong RQ. Proteomics-based identification of DEAD-box protein 48 as a novel autoantigen, a prospective serum marker for pancreatic cancer. Biochem Biophys Res Commun. 2005;330:526–32.
30. López-Cánovas JL, Hermán-Sánchez N, Moreno-Montilla MT, Del Rio-Moreno M, Alors-Perez E, Sánchez-Frias ME, et al. Spliceosomal profiling identifies EIF4A3 as a novel oncogene in hepatocellular carcinoma acting through the modulation of FGFR4 splicing. Clin Transl Med. 2022;12:e1102.
31. Liu Q, Dong H. EIF4A3-mediated hsa_circ_0088088 promotes the carcinogenesis of breast cancer by sponging miR-135-5p. J Biochem Mol Toxicol. 2021;35:e22909.
32. Yang M, Hu H, Wu S, Ding J, Yin B, Huang B, et al. EIF4A3-regulated circ_0087429 can reverse EMT and inhibit the progression of cervical cancer via miR-5003-3p-dependent upregulation of OGN expression. J Exp Clin Cancer Res. 2022;41:165.
33. Cancer Genome Atlas Research Network. Integrated genomic characterization of pancreatic ductal adenocarcinoma. Cancer Cell. 2017;32:185–203.e13.
34. Cerami E, Gao J, Dogrusoz U, Gross BE, Sumer SO, Aksoy BA, et al. The cBio cancer genomics portal: an open platform for exploring multidimensional cancer genomics data. Cancer Discov. 2012;2:401–4.
35. Gao J, Aksoy BA, Dogrusoz U, Dresdner G, Gross B, Sumer SO, et al. Integrative analysis of complex cancer genomics and clinical profiles using the cBioPortal. Sci Signal. 2013;6:pl1.
36. Uphoff CC, Drexler HG. Detection of mycoplasma contaminations. Methods Mol Biol. 2005;290:13–23.
37. Alors-Pérez E, Blázquez-Encinas R, Moreno-Montilla MT, García-Vioque V, Jiménez-Vacas JM, Mafficini A, et al. Spliceosomic dysregulation in pancreatic cancer uncovers splicing factors PRPF8 and RBMX as novel candidate actionable targets. Mol Oncol. 2024. https://doi.org/10.1002/1878-0261.13658. Online ahead of print.
38. Pedraza-Arevalo S, Alors-Pérez E, Blázquez-Encinas R, Herrera-Martínez AD, Jiménez-Vacas JM, Fuentes-Fayos AC, et al. Spliceosomic dysregulation unveils NOVA1 as a candidate actionable therapeutic target in pancreatic neuroendocrine tumors. Transl Res J Lab Clin Med. 2023;251:63–73.
39. Alors-Pérez E, Pedraza-Arevalo S, Blázquez-Encinas R, García-Vioque V, Agraz-Doblas A, Yubero-Serrano EM, et al. Altered CELF4 splicing factor enhances pancreatic neuroendocrine tumors aggressiveness influencing mTOR and everolimus response. Mol Ther Nucleic Acids. 2024;35:102090.
40. Ibáñez-Costa A, López-Sánchez LM, Gahete MD, Rivero-Cortés E, Vázquez-Borrego MC, Gálvez MA, et al. BIM-23A760 influences key functional endpoints in pituitary adenomas and normal pituitaries: molecular mechanisms underlying the differential response in adenomas. Sci Rep. 2017;7:42002.
41. Pedraza-Arevalo S, Alors-Pérez E, Blázquez-Encinas R, Herrera-Martínez AD, Jiménez-Vacas JM, Fuentes-Fayos AC. et al. Spliceosomic dysregulation unveils NOVA1 as a candidate actionable therapeutic target in pancreatic neuroendocrine tumors. Transl Res. 2023;251:63–73.
42. Hormaechea-Agulla D, Jiménez-Vacas JM, Gómez-Gómez E, L-López F, Carrasco-Valiente J, Valero-Rosa J, et al. The oncogenic role of the spliced somatostatin receptor sst5TMD4 variant in prostate cancer. FASEB J. 2017;31:4682–96.
43. Schindelin J, Arganda-Carreras I, Frise E, Kaynig V, Longair M, Pietzsch T, et al. Fiji: an open-source platform for biological-image analysis. Nat Methods. 2012;9:676–82.
44. Blázquez-Encinas R, García-Vioque V, Caro-Cuenca T, Moreno-Montilla MT, Mangili F, Alors-Pérez E, et al. Altered splicing machinery in lung carcinoids unveils NOVA1, PRPF8 and SRSF10 as novel candidates to understand tumor biology and expand biomarker discovery. J Transl Med. 2023;21:879.
45. Guillaumond F, Leca J, Olivares O, Lavaut MN, Vidal N, Berthezène P, et al. Strengthened glycolysis under hypoxia supports tumor symbiosis and hexosamine biosynthesis in pancreatic adenocarcinoma. Proc Natl Acad Sci USA. 2013;110:3919–24.
46. Schlautmann LP, Gehring NH. A day in the life of the exon junction complex. Biomolecules. 2020;10:866.
47. Seiter S, Arch R, Reber S, Komitowski D, Hofmann M, Ponta H, et al. Prevention of tumor metastasis formation by anti-variant CD44. J Exp Med. 1993;177:443–55.
48. Ma X, Li B, Liu J, Fu Y, Luo Y. Phosphoglycerate dehydrogenase promotes pancreatic cancer development by interacting with eIF4A1 and eIF4E. J Exp Clin Cancer Res. 2019;38:66.

49. Wang R, Zhang S, Chen X, Li N, Li J, Jia R, et al. EIF4A3-induced circular RNA MMP9 (circMMP9) acts as a sponge of miR-124 and promotes glioblastoma multiforme cell tumorigenesis. Mol Cancer. 2018;17:166.
50. Tang W, Wang D, Shao L, Liu X, Zheng J, Xue Y, et al. LINC00680 and TTN-AS1 stabilized by EIF4A3 promoted malignant biological behaviors of glioblastoma cells. Mol Ther Nucleic Acids. 2020;19:905–21.
51. Jiang X, Guo S, Wang S, Zhang Y, Chen H, Wang Y, et al. EIF4A3-induced circARHGAP29 promotes aerobic glycolysis in docetaxel-resistant prostate cancer through IGF2BP2/c-Myc/LDHA signaling. Cancer Res. 2022;82:831–45.
52. Ala M. Target c-Myc to treat pancreatic cancer. Cancer Biol Ther. 2022;23:34–50.
53. Wirth M, Schneider G. MYC: a stratification marker for pancreatic cancer therapy. Trends Cancer. 2016;2:1–3.
54. Schleger C, Verbeke C, Hildenbrand R, Zentgraf H, Bleyl U. c-MYC activation in primary and metastatic ductal adenocarcinoma of the pancreas: incidence, mechanisms, and clinical significance. Mod Pathol. 2002;15:462–9.
55. Urbanski L, Brugiolo M, Park S, Angarola BL, Leclair NK, Yurieva M, et al. MYC regulates a pan-cancer network of co-expressed oncogenic splicing factors. Cell Rep. 2022;41:111704.
56. Masoud R, Reyes-Castellanos G, Lac S, Garcia J, Dou S, Shintu L, et al. Targeting mitochondrial complex I overcomes chemoresistance in high OXPHOS pancreatic cancer. Cell Rep Med. 2020;1:100143.
57. Mazloomian A, Araki S, Ohori M, El-Naggar AM, Yap D, Bashashati A, et al. Pharmacological systems analysis defines EIF4A3 functions in cell-cycle and RNA stress granule formation. Commun Biol. 2019;2:1–15.
58. Egberts JH, Cloosters V, Noack A, Schniewind B, Thon L, Klose S, et al. Anti-tumor necrosis factor therapy inhibits pancreatic tumor growth and metastasis. Cancer Res. 2008;68:1443–50.
59. Tu M, Klein L, Espinet E, Georgomanolis T, Wegwitz F, Li X, et al. TNF-α-producing macrophages determine subtype identity and prognosis via AP1 enhancer reprogramming in pancreatic cancer. Nat Cancer. 2021;2:1185–203.
60. Zhao X, Fan W, Xu Z, Chen H, He Y, Yang G, et al. Inhibiting tumor necrosis factor-alpha diminishes desmoplasia and inflammation to overcome chemoresistance in pancreatic ductal adenocarcinoma. Oncotarget. 2016;7:81110–22.
61. Wang Z, Murigneux V, Le Hir H. Transcriptome-wide modulation of splicing by the exon junction complex. Genome Biol. 2014;15:551.
62. Tang Z, Li C, Kang B, Gao G, Li C, Zhang Z. GEPIA: a web server for cancer and normal gene expression profiling and interactive analyses. Nucleic Acids Res. 2017;45:W98–102.

ACKNOWLEDGEMENTS

We thank all patients and their families for generously donating the samples studies in this work.

AUTHOR CONTRIBUTIONS

All authors have read and approved the manuscript. All authors contributed to the study conception and design. Material preparation and data collection were performed by R Blázquez-Encinas, E Alors-Pérez, ME Sánchez-Frías, A Arjona-Sánchez, S Pedraza-Arevalo, A Ibáñez-Costa and JP Castaño. Experiments and analysis were performed by R Blázquez-Encinas, E Alors-Pérez, MT Moreno-Montilla and V García-Vioque. The first draft of the manuscript was written by R Blázquez-Encinas and JP Castaño and all authors commented on previous versions of the manuscript. All authors read and approved the final manuscript.

FUNDING

This work was supported by Spanish Ministry of Economy [MINECO; M (JPC)] and Ministry of Science and Innovation [MICINN; PID2019-105201RB-I00, AEI/10.13039/501100011033 (JPC)]. Instituto de Salud Carlos III, co-funded by European Union (ERDF/ESF, "Investing in your future") Predoctoral contract FI17/00282 (EAP). Society for Endocrinology Early Career Grant (AIC). Spanish Ministry of Universities Predoctoral contracts FPU18/02275 (RBE) and FPU20/03958 (VGV). Junta de Andalucía (BIO-0139); FEDER UCO-2020999019189O4 (JPC and AIC). Postdoctoral contract under the program María Zambrano funded by the European Union Next Generation-EU (SPA). Associazione Italiana Ricerca Cancro (AIRC IG n. 26343); Fondazione Italiana Malattie Pancreas—Ministero Salute [CUP J37G22000230001]; NextGenerationEU through M.U.R. under PNRR "HEAL ITALIA" n. at University of Verona, project: PE00000019, CUP: B33C22001030006 (AS). Asociación Cáncer de Páncreas (ACAPAN) and AESPANC 2022 (JPC and AIC). Grupo Español de Tumores Neuroendocrinos y Endocrinos (GETNE2016 and GETNE2019 Research grants; JPC). Fundación Eugenio Rodríguez Pascual (FERP2020 Grant; JPC). CIBERobn Fisiopatología de la Obesidad y Nutrición. CIBER is an initiative of Instituto de Salud Carlos III. Part of this work was supported by COST (European Cooperation in Science and Technology—www.cost.eu) through the COST Action TRANSPAN (CA21116).

COMPETING INTERESTS

The authors declare no competing interests.

ETHICAL APPROVAL

This study was approved by the Ethics Committee of the Reina Sofia University Hospital and the Declaration of Helsinki guidelines were followed. Informed consent documentation was obtained from each of the patients involved in the study. Mice xenograft experiments were performed according to the European-Regulations for Animal-Care under the approval of the University of Cordoba research ethics committees.

ADDITIONAL INFORMATION

Supplementary information The online version contains supplementary material available at https://doi.org/10.1038/s41417-024-00814-3.

Correspondence and requests for materials should be addressed to Alejandro Ibáñez-Costa or Justo P. Castaño.